Inorg. Chem. **2008**, *47*, 11720−11733

Organometallic and Conjugated Organic Polymers Held Together by Strong Electrostatic Interactions to Form Luminescent Hybrid Materials

Diana Bellows,[†] Émilie Gingras,[‡] Shawkat M. Aly,[†] Alaa S. Abd-El-Aziz,[§] Mario Leclerc,*[,‡] and Pierre D. Harvey*[,†]

Département de chimie, Université de Sherbrooke, Sherbrooke, Québec, Canada, J1K 2R1, Département de chimie, Université Laval, Québec, Canada G1K 7P4, and Department of Chemistry, UBC Okanagan, 3333 University Way, Kelona, BC, Canada, V1V 1V7

Received August 3, 2008

The organometallic polymers $([Ag(dmb)_2]BF_4)_n$ (dmb = 1,8-diisocyano-*p*-menthane) and $([Pt_2(dppm)_2(CNC_6Me_4NC)](BF_4)_2)_n$ (dppm = $(Ph_2P)_2CH_2$, CNC_6Me_4NC = 1,4-diisocyano-tetramethylbenzene) were reacted with the conjugated organic polymers of the type $(-Cz\text{-}C_6H_4-)_n$ and $(-Cz-)_n$, where Cz is a 2,7-linked carbazole unit substituted by $(CH_2)_3SO_3Na$ or $(CH_2)_4SO_3Na$ pendant groups at the *N*- position, to form polycation/polyanion hybrid materials. These rather insoluble and amorphous (X-ray diffraction) materials were characterized by ^1H and ^{13}C NMR MAS (magic angle spinning), solid-state IR, and Raman spectroscopy as well as chemical analyses. The hybrids exhibit fluorescence and phosphorescence arising from the polycarbazole units where evidence for a heavy atom effect is provided (Na < Ag < Pt) from the relative enhanced phosphorescence intensity, as well as triplet−triplet energy transfers from the $([Ag(dmb)_2]^+)_n$ to the polycarbazole and from the polycarbazole to the $([Pt_2(dppm)_2(CNC_6Me_4NC)]^{2+})_n$ unit. Evidence for energy transfer in these polymeric materials is provided from time-resolved emission spectroscopy, where the emission band associated with the $([Ag(dmb)_2]^+)_n$ is found to be quenched where both the relative intensity and emission lifetime exhibit a large decrease (microsecond to nanosecond time scale).

Introduction

Polycarbazoles have shown numerous applications, particularly in the area of photovoltaic cells[1] and polymer light-emitting diodes,[2] because of the possibility of light emission and good hole transport ability.[3] One of the common features in these studies is that the polycarbazoles were invariably under the form of neutral polymers. However, the possibility of combining two polymers together, adding their mutual effects on each other, opens the door to the modification of properties, including the optical and luminescence characteristics. For example, one material may emit in the blue region while the second may be luminescent in the red region of the visible spectrum, leading to combined materials capable of emitting an overall white color, potentially useful for indoor and outdoor lighting. Another example is if one polymer exhibits a high degree of self-1D-organization, hence forming highly crystalline materials; then, the second polymer would also have a tendency to align with the other, providing a mixed-polymer material with a high degree of alignment. In such a case, the rate for charge and hole transport in the material should be more efficient. One way to combine polymers in a controlled manner, such as securing a 1:1 ratio and proximity of the two polymers of the two components, is to utilize electrostatic interactions, as illustrated in Scheme 1. Strong electrostatic interactions should provide binding of a polycation with a polyanion, allowing other interactions such as a heavy atom effect and excited-state energy transfer to operate efficiently.[4] The heavy atom effect promotes population of the triplet state, hence giving rise to accentuated phosphorescence, and energy transfers are nonradiative processes that allow the harvested light

* Author to whom correspondence should be addressed. Tel.: +1-819-821-7092(P.D.H.), +1-418-656-3452(M.L.). Fax: +1-819-821-8017 (P.D.H.), +1-418-656-7916 (M.L.). E-mail:Pierre.Harvey@usherbrooke.ca (P.D.H.), mario.leclerc@chm.ulaval.ca (M.L.).
[†] Université de Sherbrooke.
[‡] Université Laval.
[§] UBC Okanagan.

(1) (a) Blouin, N.; Michaud, A.; Leclerc, M. *Adv. Mater.* **2007**, *19*, 2295. (b) Leclerc, N.; Michaud, A.; Sirois, K.; Morin, J.-F.; Leclerc, M. *Adv. Funct. Mater.* **2006**, *16*, 1694. (c) Li, J.; Dierschke, F.; Wu, J.; Grimsdale, A. C.; Muellen, K. *J. Mater. Chem.* **2006**, *16*, 96.

10.1021/ic801461j CCC: $40.75
Published on Web 11/13/2008

Scheme 1

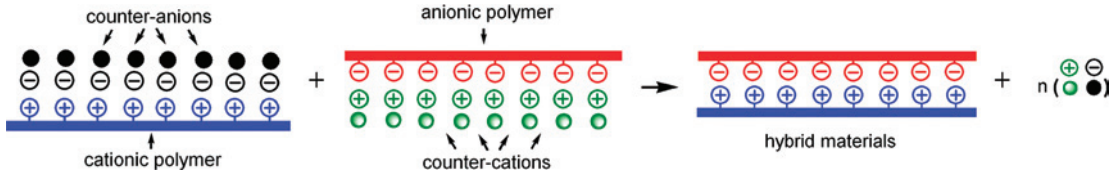

Scheme 2

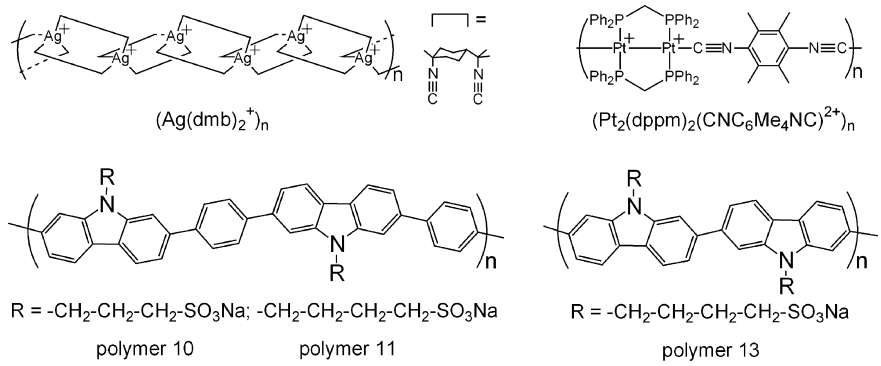

energy to flow through a material from one site to another. This process is also called the antenna effect.[4]

We now wish to report the preparation and characterization of hybrid materials composed of organometallic polymers $([Ag(dmb)_2]BF_4)_n$ and $([Pt_2(dppm)_2(CNC_6Me_4NC)](BF_4)_2)_n$ (dppm = $(Ph_2P)_2CH_2$) and conjugated organic polymers of the type $(-Cz\text{-}C_6H_4-)_n$ and $(-Cz-)_n$, where Cz is a 2,7-linked carbazole unit substituted by $(CH_2)_3SO_3Na$ or $(CH_2)_4SO_3Na$ pendant groups at the *N*- position (Scheme 2). Indeed, evidence for the heavy atom effect and triplet−triplet energy transfer will be provided.

Experimental Section

Materials. $\{[Ag(dmb)_2](BF_4)\}_n$,[5,6] $\{[Pt_2(dppm)_2(CNC_6Me_4NC)](BF_4)_2\}_n$,[7] *N*-hexyl-3,6-bisethynylcarbazole,[8] and the *N*-butylcarbazol-3,6-diyl trimer[8] were synthesized according to the literature procedures. $NaBF_4$, $AgBF_4$, and dppm were all purchased from Aldrich and used as received. All other starting products were purchased from Aldrich, Alfa Aesar, or TCI America and used without further purification. Some reaction solvents were distilled from CaH_2 before use (dichloromethane, tetrahydrofuran, triethylamine, diethyl ether, and toluene). *N*,*N*-dimethylformamide was already anhydrous. Column chromatography was carried out on silica gel (size, 40−63 μm; pore size, 60 Å; silicycle). The syntheses of 2,7-dibromo-9-H-carbazole (**1**)[9] and $PdCl_2(dppf)$[10] have already been reported in the literature. All other compounds have been synthesized following procedures described below. The solvents acetonitrile (Anachemia), diethyl ether (Fisher), acetone (ACP), dicloromethane (EMD), dimethylsulfoxide (Fisher), hexane (ACP), propanol (Fisher), and methanol (ACP) were purified according to literature procedures.[11]

Sodium 3-(2,7-Dibromocarbazole)propane-1-sulfonate (4). According to Zong and Reynolds[12] procedures, in a 100 mL flame-dried flask containing a magnetic stir bar and fit with a condenser were added 4.000 g of 2,7-dibromocarbazole (12.31 mmol) under argon, followed by two cycles of vacuum and argon. Anhydrous THF (61.5 mL) was added, and the solution was cooled to 0 °C for 15 min. Sodium hydride (0.3544 g, 14.77 mmol) was then slowly added to the solution, and it was stirred for 30 min. Finally, 1.804 g of propanesultone (14.77 mmol) was added to the reaction and refluxed overnight. The white solid was filtered, washed with acetone, and dried at ambient conditions for 30 min. The product was crystallized from water to afford 6.021 g of white powder (yield: 90%). The product has no melting point but degrades at 350 °C. ^{1}H NMR (400 MHz, DMSO-d_6, ppm): δ 8.12 (d, 2H, J_{H-H} = 8.3); 7.96 (d, 2H, J_{H-H} = 1.6); 7.36 (dd, 2H, J_{1H-H} = 8.3 and

(2) (a) Fu, Y.; Sun, M.; Wu, Y.; Bo, Z.; Ma, D. *J. Polym. Sci., Part A: Polym. Chem.* **2008**, *46* (4), 1349. (b) Wei, Z.; Xu, J.; Zeng, L.; Le, Z.; Shen, L.; Pu, S. *J. Mater. Sci.* **2008**, *43*, 1008. (c) Liu, R.; Xiong, Y.; Zeng, W.; Wu, Z.; Du, B.; Yang, W.; Sun, M.; Cao, Y. *Macromol. Chem. Phys.* **2007**, *208*, 1503. (d) Wang, H.; Ryu, J.-T.; Han, Y. S.; Kim, D.-H.; Choi, B. D.; Kwon, Y. *Mol. Cryst. Liq. Cryst.* **2007**, *463*, 285. (e) Baba, A.; Onishi, K.; Knoll, W.; Advincula, R. C. *J. Phys. Chem. B* **2004**, *108*, 18949. (f) Hameurlaine, A.; Dehaen, W.; Peng, H.; Xie, Z.; Tang, B. Z. *J. Macromol. Sci. Pure Appl. Chem.* **2004**, *A41*, 295. (g) Huang, J.; Niu, Y.; Xu, Y.; Hou, Q.; Yang, W.; Mo, Y.; Yuan, M.; Cao, Y. *Synth. Met.* **2003**, *135−136*, 181. (h) Chen, X.; Liao, J.-L.; Liang, Y.; Ahmed, M. O.; Tseng, H. E.; Chen, S. A. *J. Am. Chem. Soc.* **2003**, *125*, 636. (i) Huang, J.; Xu, Y.; Hou, Q.; Yang, W.; Yuan, M.; Cao, Y. *Institute of Polymer Optoelectronic Materials and Devices Macromolecular Rapid Communications* **2002**, *23*, 709. (j) Yapi, A. S.; Bernede, J. C.; Delvalle, M. A.; Tregouet, Y.; Ragot, F.; Diaz, F. R.; Lefrant, S. *Synth. Met.* **2002**, *126*, 1. (k) Chao, C.-S.; Whang, W.-T.; Hung, C.-H. *Macromol. Chem. Phys.* **2001**, *202*, 2864. (l) Jin, S.-H.; Kim, W.-H.; Song, I.-S.; Kwon, S.-K.; Lee, K.-S.; Han, E.-M. *Thin Solid Films* **2000**, *363*, 255. (m) Yang, Y.; Pei, Q. *Appl. Phys. Lett.* **1997**, *70*, 1926.

(3) Yavuz, O.; Ram, M. K. *Supramolecular Engineering of Conducting Materials*; Fractal System Inc.: Safety Harbor, FL, 2005; p 303.

(4) Harvey, P. D. Recent Advances in Free and Metalated Multi-Porphyrin Assemblies and Arrays; A Photophysical Behavior and Energy Transfer Perspective. In *The Porphyrin Handbook*; Kadish, K. M., Smith, K. M., Guilard, R., Eds.; Academic Press: San Diego, CA, 2003; Vol. *18*, pp 63−250.

(5) Perreault, D.; Drouin, M.; Michel, A.; Harvey, P. D. *Inorg. Chem.* **1992**, *31*, 3688.

(6) Fortin, D.; Drouin, M.; Turcotte, M.; Harvey, P. D. *J. Am. Chem. Soc.* **1997**, *119*, 531.

(7) Bérubé, J.-F.; Gagnon, K.; Fortin, D.; Decken, A.; Harvey, P. D. *Inorg. Chem.* **2006**, *45*, 2812.

(8) Aly, Sh. M.; Ho, C.-L.; Fortin, D.; Wong, W.-Y.; Abd-El-Aziz, A. S.; Harvey, P. D. *Chem.—Eur. J.* **2008**(online).

(9) Dierschke, F.; Grimsdale, A. C.; Mullen, K. *Synthesis* **2003**, 2470–2472.

(10) Hayashi, T.; Konishi, M.; Kobori, Y.; Kumada, M.; Higuchi, T.; Hirotsu, K. *J. Am. Chem. Soc.* **1984**, *106*, 158.

Table 1. Codes Employed for the Hybrid Materials

Code	Components	IR (ν(NC))/ cm^{-1}
hybrid A	polymer **10**/$([Ag(dmb)_2]BF_4)_n$	2179
hybrid B	polymer **10**/$([Pt_2(dppm)_2(CNC_{10}H_{12}NC)](BF_4)_2)_n$	2153
hybrid C	polymer **11**/$([Ag(dmb)_2]BF_4)_n$	2179
hybrid D	polymer **11**/$([Pt_2(dppm)_2(CNC_{10}H_{12}NC)](BF_4)_2)_n$	2153
hybrid E	polymer **13**/$([Ag(dmb)_2]BF_4)_n$	2184
hybrid F	polymer **13**/$([Pt_2(dppm)_2(CNC_{10}H_{12}NC)](BF_4)_2)_n$	2152

J_{2H-H} = 1.7); 4.51 (t, 2H, J_{H-H} = 7.1); 2.43 (t, 2H J_{H-H} = 7.5); 2.02 (m, 2H). ^{13}C NMR (100 MHz, DMSO-d_6, ppm): δ 141.2; 122.2; 122.2; 120.7; 119.3; 112.6; 48.4; 41.49; 24.9. IR (KBr): ν/cm^{-1} 327 (SO_2); 1188 (SO_2); 1057 (SO_3^-).

Sodium 4-(2,7-Dibromocarbazole)butane-1-sulfonate (5). According to Zong and Reynolds,[12] in a flame-dried 250 mL round-bottom flask containing a magnetic stir bar and fit with a condenser was added 7.000 g of 2,7-dibromocarbazole (21.54 mmol) under argon. Two cycles of vacuum and argon were performed. Anhydrous THF (108 mL) was added, and the solution was cooled to 0 °C for 15 min. Sodium hydride (0.5686 g, 23.69 mmol) was slowly added to the solution, and it was stirred for 30 min. Finally, 2.894 g of butanesultone (23.69 mmol) was added to the reaction, and the solution was refluxed overnight. The white solid was filtered, washed with acetone, and dried under ambient conditions for 30 min. The product was recrystallized from water to afford 9.806 g of white powder (yield: 94%). No melting point was observed, but the product degrades at 330 °C. ^{1}H NMR (400 MHz, DMSO-d_6, ppm): δ 8.12 (d, 2H, J_{H-H} = 8.3); 7.94 (d, 2H, J_{H-H} = 1.6); 7.35 (dd, 2H, J_{1H-H} = 8.3 and J_{2H-H} = 1.7); 4.39 (t, 2H, J_{H-H} = 7.3); 2.43 (t, 2H, J_{H-H} = 7.6); 1.78 (m, 2H); 1.62 (m, 2H). ^{13}C NMR (100 MHz, DMSO-d_6, ppm): δ 141.1; 122.2; 122.1; 120.7; 119.2; 112.6; 51.0; 42.4; 27.7; 22.6. IR (KBr): ν/cm^{-1} 1327 (SO_2); 1182 (SO_2); 1053 (SO_3^-).

4-(2,7-Dibromocarbazole)butane-1-sulfonyl Chloride (6). To a flame-dried 50 mL flask containing a magnetic stir bar and fit with a condenser was added 4.000 g of **5** (8.279 mmol). Three vacuum and argon cycles were performed. Phosphorus pentachloride (1.724 g, 8.279 mmol) was added followed by two argon and vacuum cycles. The reaction was heated with an oil bath to 100 °C for 2 h and to 125 °C for 12 additional hours. The reaction was cooled to room temperature, poured into 100 mL of crushed ice, and stirred for 15 min. Chloroform (100 mL) was added, and the solution was heated (~40 °C) and stirred for 30 min. The mixture was extracted three times with chloroform. The combined organic layers were dried over $MgSO_4$ and the solvent removed under reduced pressure, giving a brown oil. A minimum amount of chloroform was added to the round-bottom flask followed by approximately 200 mL of petroleum ether (until a pale brown precipitate was obtained). A dark brown solid sticking to the walls of the flask and a beige solid in suspension were observed and separated mechanically to recover only the beige solid by filtration. The product was washed two times with petroleum ether to afford 2.317 g of **6** (yield: 58%). Mp: 138−141 °C. ^{1}H NMR (400 MHz, $CDCl_3$, ppm): δ 7.91 (d, 2H, J_{H-H} = 8.2); 7.52 (d, 2H, J_{H-H} = 1.5); 7.38 (dd, 2H, J_{1H-H} = 8.3 and J_{2H-H} = 1.6); 4.30 (t, 2H, J_{H-H} = 6.6); 3.65 (t, 2H, J_{H-H} = 6.9); 2.11 (m, 4H). ^{13}C NMR (100 MHz, $CDCl_3$, ppm): δ 141.2; 123.2; 121.9; 121.6; 120.2; 111.8; 64.9; 42.6; 27.0; 22.4. HRMS calculated for $C_{16}H_{14}Br_2ClNO_2S$: 476.8800. Found: 476.8792 ± 0.0014.

1-Methoxy-4-octylbenzene (7). In a 1 L three-neck flame-dried round-bottom flask fit with an addition funnel and a condenser, *p*-bromoanisole (10.00 g, 53.46 mmol, and 6.69 mL) was dissolved in 214 mL of anhydrous diethyl ether and cooled to 0 °C. After 5 min, $PdCl_2$(dppf) (0.7824 g, 1.0692 mmol) was added, and the solution was stirred for 3 min. Octylmagnesium bromide (69.50 mmol, 69.50 mL of a solution of a 1 M solution in anhydrous diethyl ether) was added dropwise via the addition funnel. The reaction mixture was stirred overnight at ambient temperature under argon. The reaction was then cooled to 0 °C and slowly quenched by the addition of a solution of 10% HCl. This solution was transferred to a separatory funnel and extracted three times with ether and a saturated solution of $NaHCO_3$. The combined organic layers were then washed twice with water, dried over $MgSO_4$, and evaporated under a vacuum. The crude product was dissolved in hexane and filtered over silica, and the filtrate was evaporated. The product was distilled under reduced pressure, and the final product was recovered. The reaction affords 3.000 g of colorless oil with a yield of 25%. ^{1}H NMR (400 MHz, $CDCl_3$, ppm): δ 7.12 (d, 2H, J_{H-H} = 8.3); 6.85 (d, 2H, J_{H-H} = 8.6); 3.81 (s, 3H); 2.57 (t, 2H, J_{H-H} = 7.6); 1.61 (m, 2H); 1.31 (m, 10H); 0.92 (t, 3H, J_{H-H} = 6.8). ^{13}C NMR (100 MHz, $CDCl_3$, ppm): δ 157.7; 135.2; 129.4; 113.8; 55.4; 55.4; 35.2; 32.0; 31.9; 29.6; 29.4; 22.8; 14.3. HRMS calculated for $C_{15}H_{24}O$: 220.1827. Found: 220.1830 ± 0.0007.

4-Octylphenol (8). To a 250 mL flame-dried three-neck round-bottom flask fit with an addition funnel was added **7** (2.990 g, 13.57 mmol). The product, under argon, was solubilized in 136 mL of anhydrous dichloromethane (DCM), and the solution was cooled to −78 °C. The solution of boron tribromide (1 M in dichloromethane; 33.9 mL) was added dropwise via the addition funnel over 30 min, and the resulting solution was kept at −78 °C for 3 h. The mixture was then brought to room temperature and stirred overnight. The reaction was quenched with a solution of 10% HCl, followed by an extraction with DCM and water (three times). The combined organic layers were washed once with water and dried over $MgSO_4$. The brown oil product was solubilized in DCM and filtered over silica, and the silica pad was washed many times with DCM. The filtrate was evaporated under reduced pressure, and the final product was recrystallized easily from cold hexane. The final product was filtered and washed with hexane at 0 °C to afford 1.707 g of white crystals in a 61% yield. Mp: 38−40 °C. ^{1}H NMR (400 MHz, $CDCl_3$, ppm): δ 7.04 (d, 2H, J_{H-H} = 8.3); 6.75 (d, 2H, J_{H-H} = 8.5); 4.59 (s, 1H); 2.53 (t, 2H, J_{H-H} = 7.6); 1.56 (m, 2H); 1.28 (m, 10H); 0.88 (t, 3H, J_{H-H} = 7.0). ^{13}C NMR (100 MHz, $CDCl_3$, ppm): δ 153.5; 135.4; 129.6; 115.2; 35.2; 32.0; 31.9; 29.63; 29.4; 29.4; 22.8; 14.3. HRMS calculated for $C_{14}H_{22}O$: 206.1671. Found: 206.1679 ± 0.0006.

***p*-Octylphenyl-4-(2,7-dibromocarbazole)butane-1-sulfonate (9).** In a 100 mL round-bottom flask, flame-dried and under argon, were added 2.000 g of **6** (4.170 mmol) and 1.033 g of **8** (5.004 mmol), and these were solubilized in 42 mL of anhydrous DCM. To this solution was slowly added 2.30 mL of triethylamine (16.68 mmol), and the mixture was stirred at room temperature overnight. The reaction was controlled by thin layer chromatography (85% hexanes/15% ethyl acetate as eluent). The reaction solution was extracted three times with DCM, and the combined organic layers were subsequently washed once with water and dried over $MgSO_4$. The crude product was purified by silica-gel column chromatography (85% hexanes/15% ethyl acetate as eluent) to give 0.7701 g of pure white powder (yield:

(11) (a) Perrin, D. D.; Armarego, W. L. F.; Perrin, D. R. *Purifications of laboratory chemicals*; Pergamon Press: Oxford, 1966. (b) Gordon, A. J.; Ford, R. A. *The chemist's companion, a handbook of practical data, techniques, and references*; Wiley: New York, 1972; p 436.

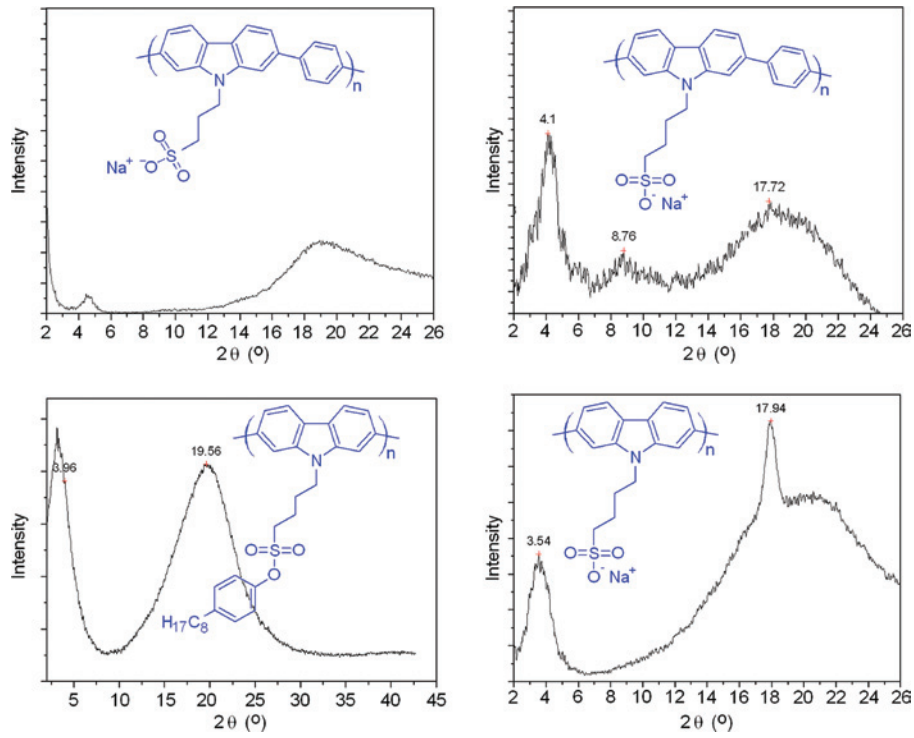

Figure 1. XRD traces for polymers **10**−**13**.

Scheme 3

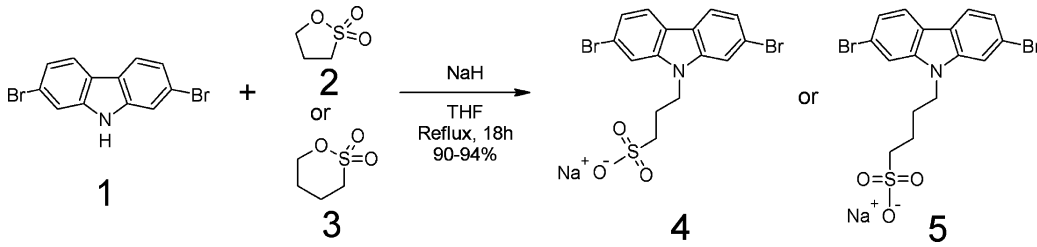

Scheme 4

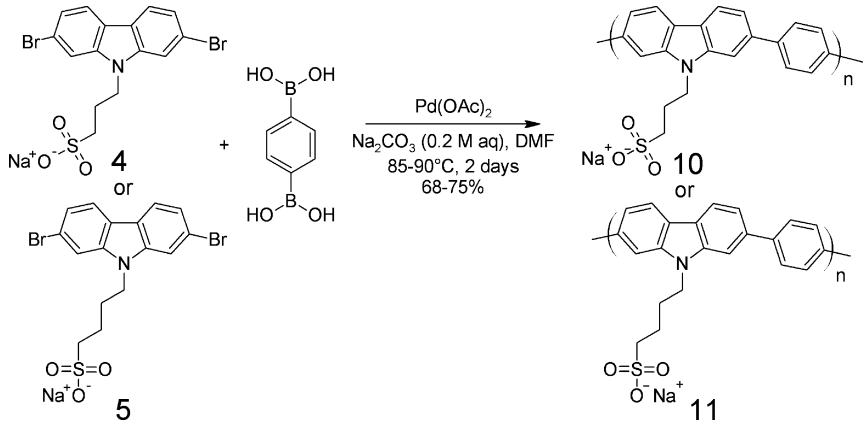

30%). Mp: 80−83 °C. ^{1}H NMR (400 MHz, $CDCl_3$, ppm): δ 7.89 (dd, 2H, J_{1H-H} = 8.2 and J_{2H-H} = 2.0); 7.52 (s, 2H); 7.36 (d, 2H, J_{H-H} = 8.1); 7.17 (dd, 2H, J_{1H-H} = 8.5 and J_{2H-H} = 1.8); 7.06 (dd, 2H, J_{1H-H} = 8.5 and J_{2H-H} = 1.8); 4.27 (t, 2H, J_{H-H} = 6.0); 3.22 (t, 2H, J_{H-H} = 6.5); 2.58 (t, 2H, J_{H-H} = 7.5); 2.05 (m, 4H); 1.58 (m, 2H); 1.28 (m, 10H); 0.88 (t, 3H, J_{H-H} = 7.0). ^{13}C NMR (100 MHz, $CDCl_3$, ppm): δ 146.9; 142.3; 141.1; 129.9; 122.9; 121.6 (2C); 121.4; 119.9; 111.8; 49.8; 42.5; 35.4; 31.9; 31.4; 29.5; 29.3; 29.3; 27.3; 22.7; 21.4; 14.2. HRMS calculated for $C_{30}H_{35}Br_2NO_3S$: 647.0704. Found: 647.0712 ± 0.0019.

Sodium Poly[N-propane-3′-sulfonate-2,7-carbazole-alt-1,4-phenylene] (10). In a 100 mL round-bottom flask, fit with a condenser and flame-dried, were added sodium 3-(2,7-dibromocarbazole)propane-1-sulfonate (**4**; 0.5000 g, 1.066 mmol), *p*-phenyldiboronic acid (1.766 g, 1.066 mmol); and palladium(II) acetate (0.0072 g, 0.0320

(12) Zong, K.; Reynolds, J. R. *J. Org. Chem.* **2001**, *66*, 6873.

Scheme 5

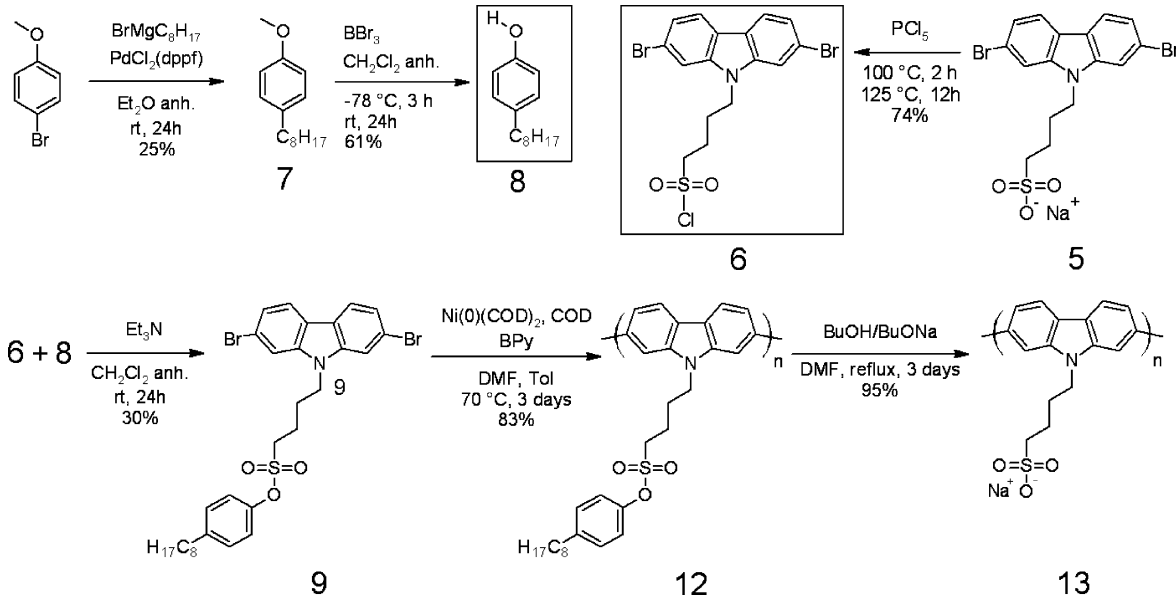

Scheme 6

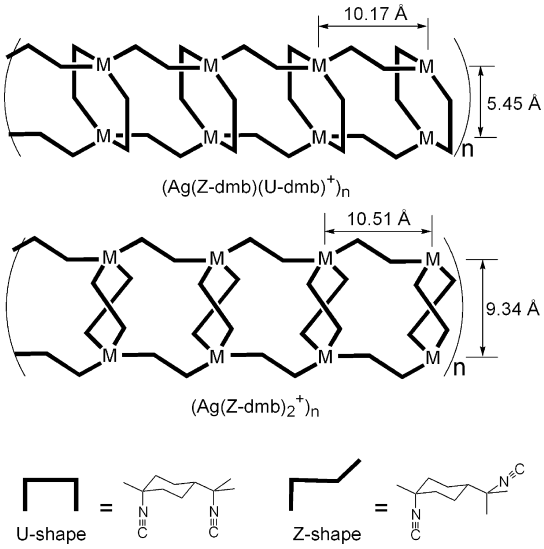

Scheme 7

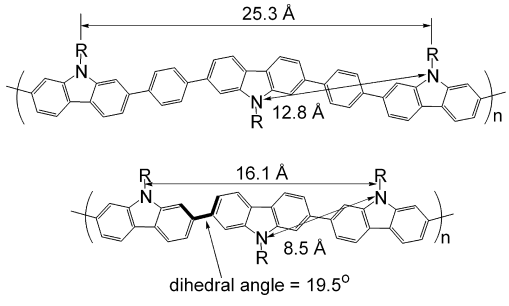

mmol) under argon. The flask was evacuated and backfilled with argon three times. In a 250 mL, flame-dried, round-bottom flask, a solution of DMF (60 mL) and aqueous Na_2CO_3 (0.2 M, 140 mL) was degassed for 30 min with argon. This solution (65 mL) was added to the first flask, and the reaction was stirred for three days at a temperature between 85 and 90 °C. After three days, the polymer was end-capped by the addition of bromobenzene (1.066 mmol, 0.25 mL), stirred for 4 h, and followed by the addition of phenylboronic acid (0.1430 g, 1.066 mmol). The resulting mixture was stirred overnight and precipitated in acetone (600 mL) in a PTFE beaker. The precipitate was filtered through a 0.45 μm PTFE membrane. The recuperated solid was suspended in water (approximately 2 mg/mL) and dialyzed for three days (MWCO 6 kDa−8 kDa) in deionized water. After dialysis, the polymer was precipitated a second time in acetone and filtered over a 0.45 μm 66-nylon membrane. A yellow to green powder was recovered (0.2750 g) with a yield of 68%. The fluorescence quantum yield of this polymer is (ϕ_{fluo}) 79% (DMSO). IR (KBr): ν/cm^{-1} 1327 (SO_2); 1184 (SO_2); 1045 (SO_3^-).

Sodium Poly[N-butane-4′-sulfonate-2,7-carbazole-alt-1,4-phenylene] (11). In a 100 mL round-bottom flask, fit with a condenser and flame-dried, were added sodium 4-(2,7-dibromocarbazole)butane-1-sulfonate (**5**; 0.5149 g, 1.066 mmol), *p*-phenyldiboronic acid (1.766 g, 1.066 mmol); and palladium(II) acetate (0.0072 g, 0.0320 mmol) under argon. The flask was evacuated and backfilled with argon three times. In another flame-dried 250 mL round-bottom flask was degassed a solution of DMF (60 mL) and aqueous Na_2CO_3 (0.2 M, 140 mL) for 30 min with argon. Then, 65 mL of this solution was added to the first flask, and the reaction was stirred for three days at a temperature of 85−90 °C. After three days, the polymer was end-capped by the addition of bromobenzene (0.5330 mmol, 0.13 mL), stirred for 4 h, and followed by the addition of phenylboronic acid (0.0715 g, 0.5330 mmol). The resulting mixture was stirred overnight and precipitated in acetone (600 mL) in a PTFE beaker. The precipitate was filtered through a 0.45 μm PTFE membrane. The recovered solid was suspended in water (approximately 2 mg/mL) and dialyzed for three days (MWCO 6 kDa−8 kDa) in deionized water. After dialysis, the polymer was precipitated a second time in acetone and filtered over a 0.45 μm 66-nylon membrane. A yellow to brown powder was recovered (0.3000 g) with a yield of 75%. The product has a fluorescence quantum yield (ϕ_{fluo}) of 80% (DMSO). IR (KBr): ν/cm^{-1} 1327 (SO_2); 1175 (SO_2); 1043 (SO_3^-).

Poly[N-butane-4′-(*p*-octylphenyl)sulfonate-2,7-carbazole] (12). In a 100 mL three-necked, flame-dried, round-bottom flask, fit with a thermometer and a condenser, were added 2,2′-dipyridyl (0.2886 g, 1.848 mmol) and bis(1,5-cyclooctadiene)nickel(0) (0.5082 g, 1.848 mmol), followed two times by an alternation between a

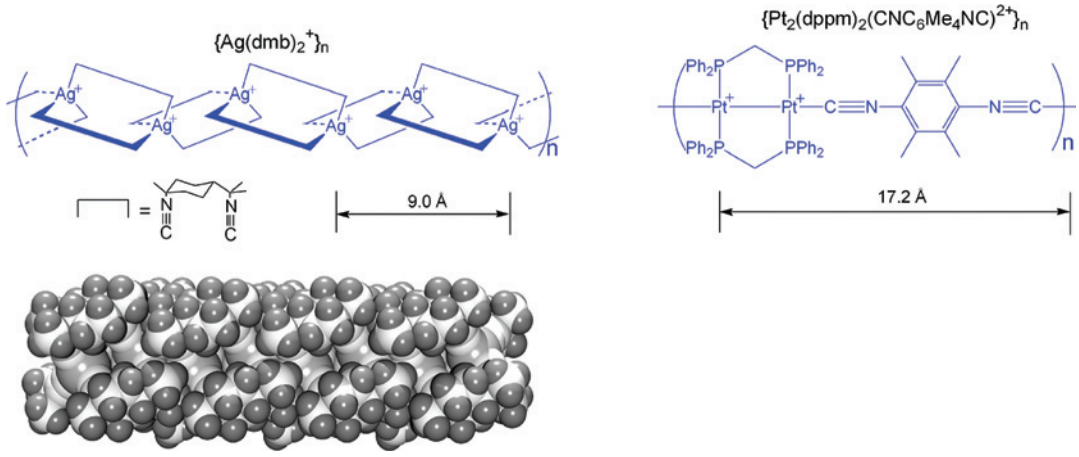

Figure 2. (Top) Drawings of the cationic $([Ag(dmb)_2]^+)_n$ and $([Pt_2(dppm)_2(CNC_6Me_4NC)]^{2+})_n$ polymers stressing the distance between repetitive units containing two positive charges. (Bottom) Space-filling model based on the X-ray structure of the $([Ag(dmb)_2]^+)_n$ polymer showing the head-to-tail symmetry of the rigid rod induced by the dmb ligand.

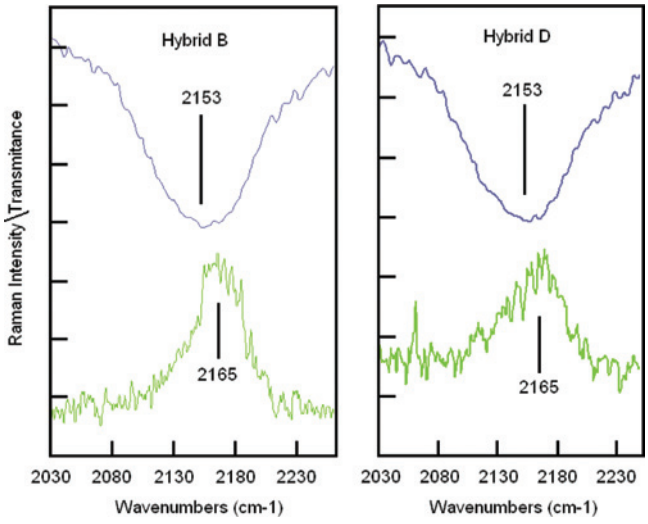

Figure 3. IR and Raman spectra of hybrids **B** and **D** in the solid state in the ν(CN) region. The fwhm are for hybrid **B** 50 and 100, and for hybrid **D** 42 and 90 cm^{-1}, for the Raman and IR peaks, respectively.

vacuum and argon. 1,5-Cyclooctadiene (1.848 mmol, 0.23 mL) was then added. Anhydrous solvents (DMF (9.6 mL) and toluene (9.6 mL)) were degassed via three freeze−pump−thaw cycles and were then added to the flask. This mixture was stirred for 30 min at 65 °C. In another flame-dried round-bottom flask filled with argon was added the monomer (*p*-octylphenyl-4-(2,7-dibromocarbazole)butane-1-sulfonate (**9**), 0.5000 g, 0.7698 mmol), and it was dissolved in degassed anhydrous toluene (19 mL). This solution was then added to the three-necked flask charged with the catalyst blend. The resulting solution was stirred under argon at 65 °C in the absence of light. After three days, the polymer was end-capped with bromobenzene (0.7698 mmol, 0.08 mL) and stirred overnight. The polymer was precipitated with MeOH/HCl (80:20) and filtered on a 0.45 μm PTFE membrane. A first Soxhlet was done in acetone and a second in DMF to dissolve the entire polymer. The DMF and polymer solution was evaporated to a minimal volume, and the solution was precipitated in a solution of MeOH/HCl (90:10). The solution was filtered on the same membrane to give a yellow-reddish powder (0.3131 g, 83%). The product has a fluorescence quantum yield (ϕ_{fluo}) of 70% (DMF). IR (KBr): ν/cm^{-1} 1327 (SO_2); 1146 s (SO_2).

Sodium Poly[N-butane-4′-sulfonate-2,7-carbazole] (13). This reaction is known as saponification. The solution of polymer (0.2500 g, 0.5100 mmol) in DMF was refluxed for 1 day in a 250 mL flame-dried round-bottom flask to ensure complete polymer dissolution. A solution of BuOH/BuONa (NaOH (0.6250 g, 15.60 mmol) in BuOH (60 mL)) was added to the first one, and the resulting mixture was refluxed for an additional three days. When the reaction was complete, $NaHCO_3$ (1.750 g, 20.80 mmol) was added, followed by filtration through a 0.45 μm PTFE membrane. The polymer was recovered as a brown powder with a yield of 95%. The fluorescence quantum yield (ϕ_{fluo}) of **13** is 84% (DMSO). IR (KBr): ν/cm^{-1} 1321 (SO_2); 1200 (SO_2); 1043 (SO_3^-).

This section describes the synthesis and characterization of the hybrid materials. The codes of these hybrids are placed in Table 1.

Hybrid Materials (A, C, E): $([Ag(dmb)_2]^+)_n$/Polycarbazoles. All three hybrid materials composed of $([Ag(dmb)_2]^+)_n$ and the conjugated polycarbazoles were prepared in a similar manner. One example is shown below.

Polymer **10** (0.0475 g, 0.0825 mmol) was placed in a 250 mL round-bottom flask and dissolved in a minimum amount of hot DMSO. The $\{[Ag(dmb)_2]BF_4\}_n$ polymer (0.0318 g, 0.0825 mmol) was dissolved in a minimum amount of acetonitrile and added dropwise to the carbazole containing polymer/dimethylsulfoxide mixture and left to react for two days. A yellow gel suspension was formed. The reaction solution was added dropwise to a beaker containing 100 mL of propanol and was precipitated with hexane. The solvent was decanted as much as possible. The same process was repeated until all of the dimethylsulfoxide was removed. The solvent remaining with the product was evaporated under a vacuum and the product washed with 20 mL of methanol several times. The product was then dried under a vacuum.

Polymer 10/$([Ag(dmb)_2]BF_4)_n$ (Hybrid A). Yield: 53% (0.072 mg). Solid-state ^{1}H NMR (MAS): δ 7.81 (aro. of the carbazole), 3.98 (CH_2(S)), 2.32 (aliphatic (dmb)). Solid-state ^{13}C NMR (MAS): δ 206.08, 193.58, 186.90, 173.54, 141.10, 138.32, 127.45, 121.49, 106.75, 62.11, 60.85, 49.29, 41.71, 35.60, 26.43, 22.28. Anal. calcd for $AgC_{45}H_{34}N_3SO_3$ (804.70): C, 67.17; H, 4.26; N, 5.22; S, 3.98. Found: C, 66.92; H, 4.04; N, 5.56; S, 4.11.

Polymer 11/$([Ag(dmb)_2]BF_4)_n$ (Hybrid C). Yield: 67% (0.054 mg). Solid-state ^{1}H NMR (MAS): δ 7.59 (aro. of the carbazole), 4.02 (CH_2(S)), 2.21 (aliphatic (dmb)). Solid-state ^{13}C NMR (MAS): δ 205.03, 193.36, 186.65, 173.18, 141.51, 138.55, 127.68, 121.57, 117.78, 106.98, 63.09, 60.75, 51.54, 42.66,

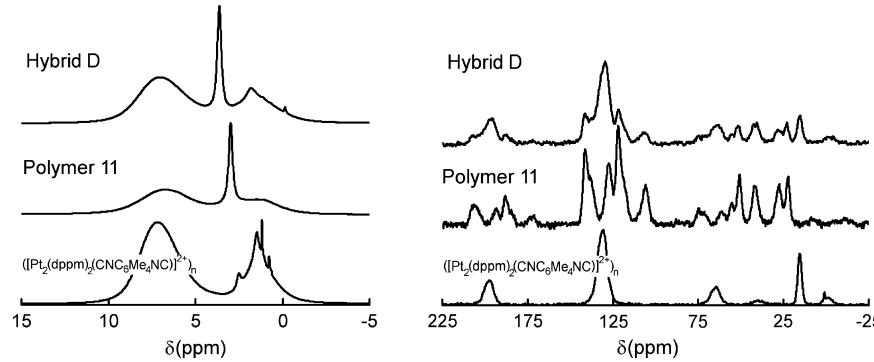

Figure 4. Comparison of the ^{1}H (left) and ^{13}C (right) NMR MAS spectra of solid $([Pt_2(dppm)_2\text{-}(CNC_6Me_4NC)](BF_4)_2)_n$, polymer **11**, and hybrid **D** at 298 K as an example.

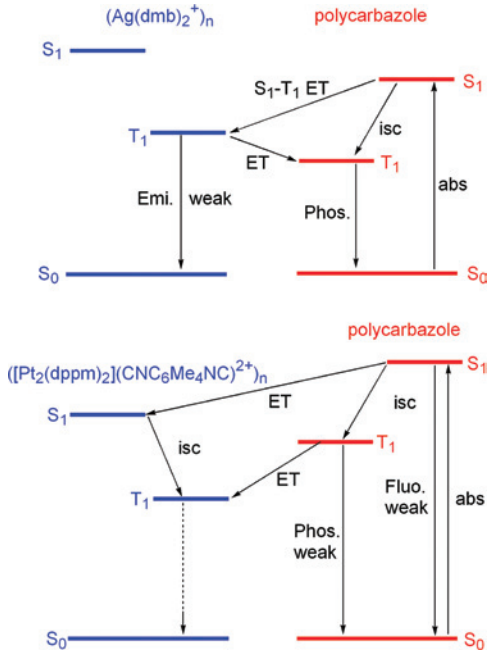

Figure 5. Energy diagram for the hybrid materials based on the observed fluorescence and phosphorescence spectra of the polycarbazole materials and the literature data for the $([Ag(dmb)_2]^+)_n$ (top) and $([Pt_2(dppm)_2](CNC_6Me_4NC)^{2+})_n$ (bottom) organometallic polymers. The exact location of the S_1 state is not known with certainty, but arguments are provided in the text in favor of this diagram where S_1 is an optically silent state (from a forbidden transition).

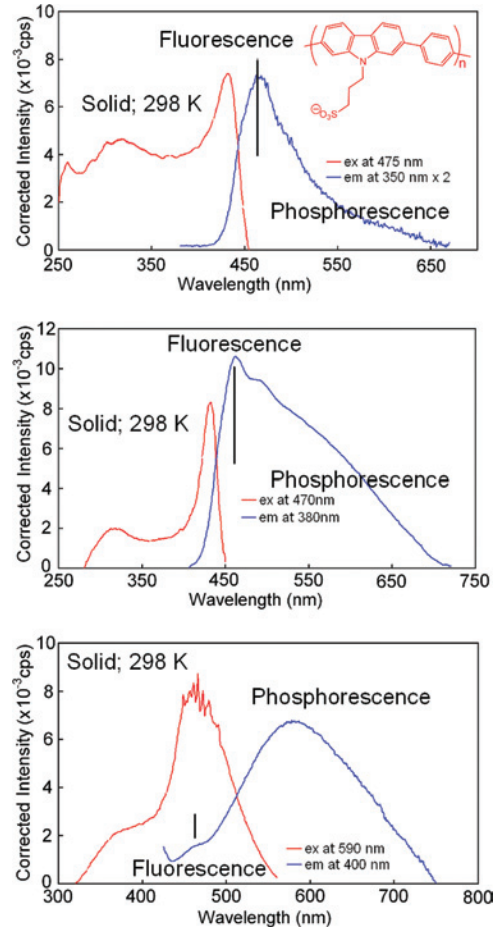

Figure 6. Solid-state excitation (red) and emission spectra (blue) of polymer **10** and hybrids **A** and **B** at 298 K. The excitation and emission wavelength are indicated in the spectra.

40.34, 35.72, 27.38, 22.29. Anal. calcd for $AgC_{46}H_{36}N_3SO_3$ (818.73): C, 67.48; H, 4.43; N, 5.13; S, 3.92. Found: C, 67.16; H, 4.17; N, 4.88; S, 3.56.

Polymer 13/$([Ag(dmb)_2]BF_4)_n$ (Hybrid E). Yield: 62% (0.119 mg). Solid-state ^{1}H NMR (MAS): δ 8.04 (aro. of the carbazole), 4.08 (CH_2(S)), 2.32 (aliphatic (dmb). Solid-state ^{13}C NMR (MAS): δ 207.74, 187.84, 173.11, 141.95, 122.01, 108.11, 63.84, 61.02, 52.57, 43.18, 40.80, 36.14, 27.76, 22.74. Anal. calcd for $AgC_{40}H_{32}N_3SO_3$ (742.63): C, 64.69; H, 4.34; N, 5.66; S, 4.32. Found: C, 65.02; H, 4.42; N, 5.21; S, 3.97.

Hybrid Materials (B, D, F): $([Pt_2(dppm)_2](CNC_6Me_4NC)]^{2+})_n$/ Polycarbazoles. All three hybrid materials composed of $([Pt_2(dppm)_2(CNC_6Me_4NC)](BF_4)_2)_n$ and the conjugated polycarbazoles were prepared in a similar manner. One example is shown below.

Polymer **11** (0.0111 g, 0.0277 mmol) was placed in a 250 mL round-bottomed flask and dissolved in a minimum amount of hot dimethylsulfoxide. The $\{[Pt_2(dppm)_2(CN\text{-}C_{10}H_{12}\text{-}NC)](BF_4)_2\}_n$ polymer (0.0200 g, 0.0139 mmol) was dissolved in a minimum amount of acetonitrile and added dropwise to the carbazole-containing polymer/dimethylsulfoxide mixture and left to react for two days. A yellow gel suspension was formed. The reaction solution was added dropwise to a beaker containing 100 mL of propanol and was precipitated with hexane. The solvent was decanted as much as possible. The same process was repeated until all of the dimethylsulfoxide was removed. The solvent remaining with the product was evaporated under a vacuum and the product washed with 20 mL of methanol several times. The product was then dried under a vacuum.

Polymer 10/$([Pt_2(dppm)_2(CNC_{10}H_{12}NC)](BF_4)_2)_n$ (Hybrid B). Yield: 66% (0.127 mg). Solid-state ^{1}H NMR (MAS): δ 7.21 (aro. from (dppm) + carbazole), 3.74 (CH_2(S)), 2.06 (aliphatic of (dppm)). Solid-state ^{13}C NMR (MAS): δ 196.26, 141.28, 137.60, 130.09, 121.53,

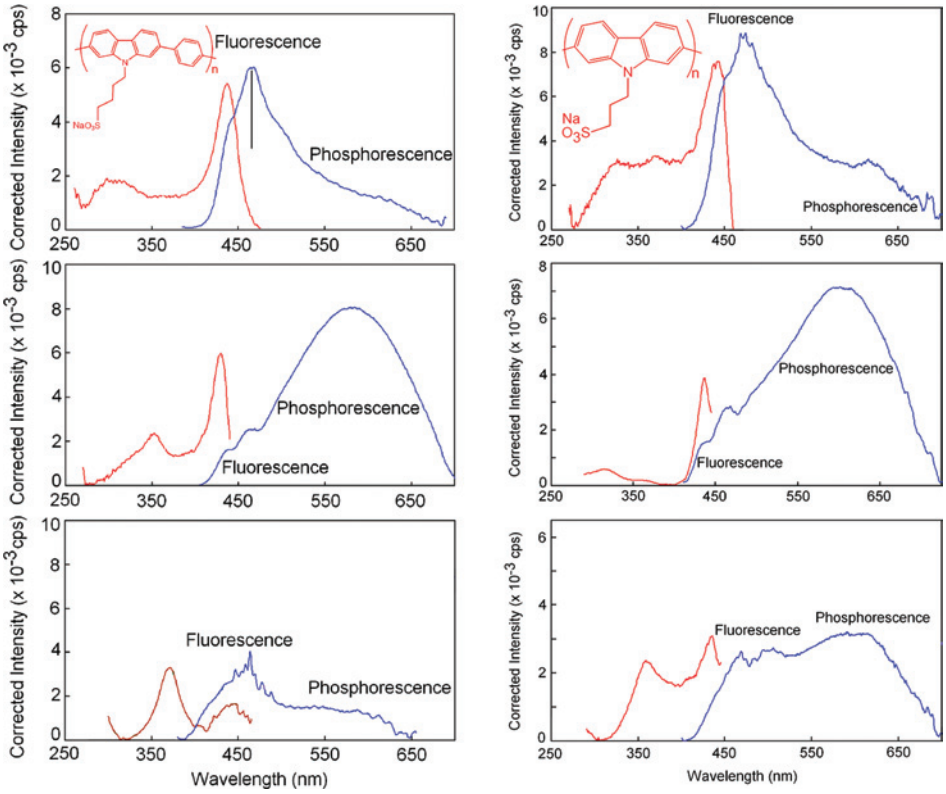

Figure 7. Solid-state excitation (red) and emission spectra (blue) of polymer **11** and hybrids **C** and **D** (left) and polymer **12** and hybrids **E** and **F** at 298 K. The excitation and emission wavelengths are 350 and 500 nm. The intensities were adjusted so that they fit in the frame. The emission intensity of the fluorescence and phosphorescence of hybrids **D** and **F** is very low.

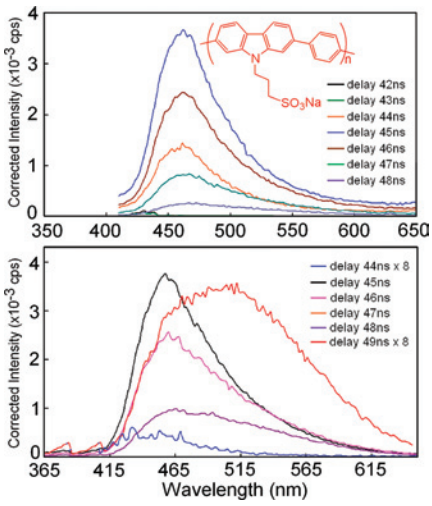

Figure 8. Time-resolved emission spectra of polymer **10** (top) and hybrid **A** (bottom) on the nanosecond time scale. The delay times labeled 42 and 43 ns are located on the short-time side of the laser pulse where the laser has not fired (fwhm = 1.4 ns). The 45 ns delay time is located at the maximum of the pulse, so the 43−45 ns delay range represents the rise time of the laser pulse. The feature is the 515-nm band associated with the emission of the $([Ag(dmb)_2]^+)_n$.

107.29, 50.01, 42.03, 40.77, 25.89, 15.45. Raman (solid): 2165 cm^{-1}. Anal. calcd for $Pt_2C_{104}H_{88}N_4S_2O_6P_4$ (2068.18): C, 60.40; H, 4.29; N, 2.71; S, 3.10. Found: C, 60.22; H, 4.10; N, 2.45; S, 2.91.

Polymer 11/$([Pt_2(dppm)_2(CNC_{10}H_{12}NC)](BF_4)_2)_n$ (Hybrid D). Yield: 56% (0.046 mg). Solid-state ^{1}H NMR: δ 7.02 (aro. from (dppm) + carbazole), 3.63 (CH_2(S)), 1.81 (aliphatic of (dppm)). Solid-state ^{13}C NMR: δ 206.98, 196.15, 187.62, 141.22, 129.63, 121.50, 106.62,

Scheme 8

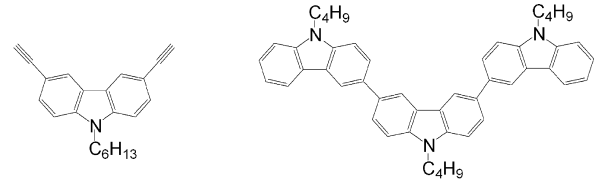

N-hexyl-3,6-bisethynylcarbazole N-butylcarbazol-3,6-diyl trimer

51.87, 41.64, 28.43, 23.08, 15.32. Raman (solid): 2165 cm^{-1}. Anal. calcd for $Pt_2C_{106}H_{92}N_4S_2O_6P_4$ (2096.07): C, 60.74; H, 4.42; N, 2.67; S, 3.06. Found: C, 60.43; H, 4.19; N, 2.39; S, 2.72.

Polymer 13/$([Pt_2(dppm)_2(CNC_{10}H_{12}NC)](BF_4)_2)_n$ (Hybrid F). Yield: 61% (0.034 mg). Solid-state ^{1}H NMR: δ 7.05 (aro. from (dppm) + carbazole), 3.73 (CH_2(S)), 1.25 (aliphatic of (dppm)). Solid-state ^{13}C NMR (MAS): δ 206.98, 196.15, 187.62, 141.84, 130.75, 121.98, 107.64, 52.24, 42.53, 29.31, 23.57, 15.73.

Apparatus. All carbazole polymers and their starting materials were characterized by NMR spectroscopy. ^{1}H and ^{13}C NMR spectra were recorded on a Varian AS400 apparatus in the mentioned deuterated solvent solution at 298 K unless otherwise specified. Chemical shifts were reported as δ values (ppm) relative to internal tetramethylsilane. All hybrid polymers were characterized by solid-state NMR spectroscopy. ^{1}H MAS and ^{13}C CP/MAS NMR experiments were performed at the National Ultrahigh-field NMR Facility for Solids (Ottawa, Canada) on a Bruker Avance II NMR spectrometer operating at 21.1 T. A double-resonance 3.2 mm Bruker probe with magic angle spinning, MAS, was used. ^{1}H and ^{13}C NMR chemical shifts were referenced to neat TMS using adamantane as a secondary chemical shift reference. ^{1}H MAS NMR spectra were recorded at a resonance frequency of 900.2 MHz. Samples were spun at a spinning speed of 20 kHz on 3.2 mm o.d.

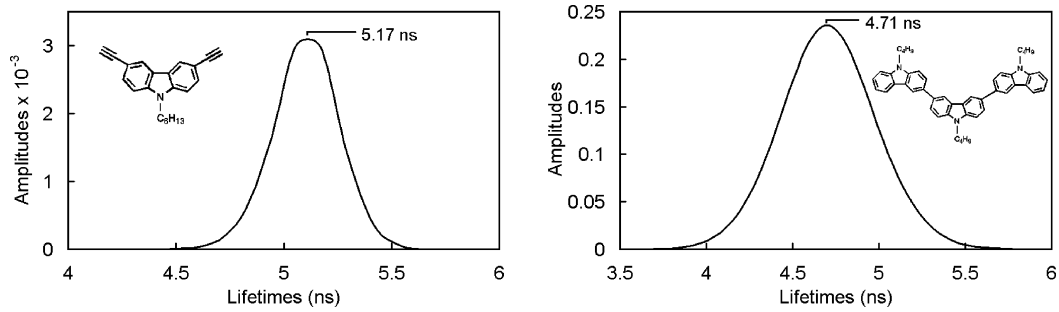

Figure 9. Fluorescence lifetime of *N*-hexyl-3,6-bisethynylcarbazole (left) and *N*-butylcarbazol-3,6-diyl trimer (right) as a solid at 298 K measured using λ_{em} = 420 nm and λ_{ex} = 350 nm.

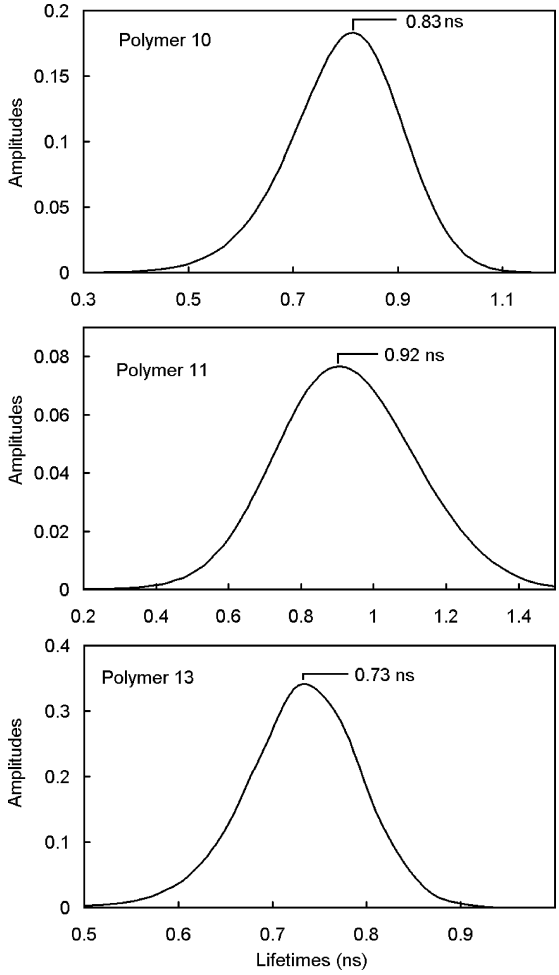

Figure 10. Distribution of fluorescence lifetimes for thin films of polymers **10**, **11**, and **13** at 298 K using λ_{em} = 460 nm and λ_{ex} = 400 nm.

ZrO_2 rotors. A single pulse sequence with background suppression was used in ^{1}H NMR experiments with an r.f. pulse length of 2.5 mks (π/2 pulse) and a 10 s relaxation delay between pulses, which was found sufficient for a complete relaxation. A total of 64 scans were accumulated in each ^{1}H NMR experiment. ^{13}C CP/MAS NMR spectra were recorded at a resonance frequency of 226.4 MHz under 15 kHz MAS. The CP contact time in all experiments was 1 ms, and a 5 s relaxation delay existed between pulses. From 2000 to 10 000 scans were accumulated in ^{13}C CP/MAS NMR experiments, depending on the amount of sample available. SPINAL-64 proton decoupling was employed during spectra acquisition.

Infrared spectra of all carbazole polymers and their starting materials were obtained on a Bomem FT-IR instrument from the MB series spectrometer on pressed, thin transparent disks of the products mixed with dried KBr. The IR spectra of the hybrid polymers were acquired on a Bomem FT-IR MB series spectrometer equipped with a baseline-diffused reflectance. FT-Raman spectra were acquired on a Bruker RFS 100/S spectrometer.

The fluorescence quantum yields of the carbazole polymers were measured on a Varian Eclipse spectrophotometer, in the mentioned optical-grade solvent degassed with argon for 5 min, with 9,10-diphenylanthracene in cyclohexane (ϕ_f = 90%) as a reference.[13] All photophysical measurements for the hybrid polymers were preformed in the following manner. The solid samples were placed in a metallic cell connected to a vacuum pump using a cell holder adjusted at a right angle, and the corrected emission and excitation spectra were obtained using a double monochromator Fluorolog II instrument from Spex. For the 77 K measurements, the cell was evacuated from the air and left for about 15 min after the addition of liquid nitrogen prior to measurements. Emission lifetimes and time-resolved spectra were measured on a TimeMaster Model TM-3/2003 apparatus from PTI. The source was a nitrogen laser with a high-resolution dye laser (fwhm $\sim$ 1400 ps), and the fluorescence lifetimes were obtained from deconvolution or distribution lifetime analysis, and the uncertainties were about 100 ps. Some of phosphorescence lifetimes were acquired on a PTI LS-100 phosphorimeter system using a 1 μs tungsten-flash lamp.

Wide-angle X-ray diffraction was performed on a Siemens/Bruker X-ray diffractometer, and the instrument used graphite monochromatized copper radiation (K = 1.5418 Å). The apparatus is a Kristalloflex 760 generator, three-circle goniometer, and Hi-Star area detector, and it is equipped with the GADDS software. The diffractometer operation power is 40 kV and 40 mA, and the collimator was 0.8 mm. The glass capillary tubes have a wall thickness of 0.01 mm and a total diameter of 1 mm.

Results and Discussion

1. Syntheses of the Anionic Carbazole-Containing Polymers. The target anionic carbazole-containing polymers are of two types. The first one contains a 1,4-C_6H_4 spacer between the carbazole units, whereas the second type is a pure homopolymer. The presence of the spacer has the effect of increasing the average distance between the anion centers on the main chain. In addition, the carbazoyl−phenylene copolymers exhibit either a 3-carbon or a 4-carbon flexible chain linking the sulfonate function to the main chain. These side chains have two roles. The first one is to act as soluble chain for characterization purposes, and the second is to investigate the effect of the chain length on the interchain interactions.

(13) Eaton, D. F. *Pure Appl. Chem.* **1988**, *60*, 1107.

Table 2. Solid-State Spectroscopic and Fluorescence Lifetime Data at 298 K

material	λ_{em} (nm)solid state	solid state (λ_{em} = 460nm)τ_F (ns); fwhm (ns)
N-hexyl-3,6-bisethynyl-carbazole	420, 460 sh	5.17;[a] 0.355
N-butylcarbazol-3,6-diyl trimer	430, 460 sh	4.71;[a] 0.66
polymer **10**	400, 465, 495 sh	0.83; 0.26
hybrid **A**	400, 463, 492, 550sh	0.92; 0.32
hybrid **B**	397, 468sh, 580	1.18; 0.36
polymer **11**	397, 443sh, 467, 495sh, 615sh	0.92; 0.48
hybrid **C**	395, 437sh, 464 sh, 580	0.80; 0.17
hybrid **D**	395, 460, 585	0.80; 0.14
polymer **13**	395, 451sh, 471, 500sh, 617sh	0.73; 0.14
hybrid **E**	397, 437sh, 470, 607 broad	0.49; 0.17
hybrid **F**	397, 470, 495, 595	0.75; 0.31

[a] λ_{em} = 420 nm and λ_{ex} = 350 nm.

Table 3. Phosphorescence Lifetimes Measured As Solid Suspended in Frozen 2MeTHF at 77 K Using λ_{ex} = 450 nm and Monitored at λ_{em} = 600 nm

	%	τ (ms)	χ^a		%	τ (ms)	χ^a
polymer **10**	47	0.627 ± 0.009	0.795	hybrid **C**	60	0.816 ± 0.149	1.067
	20	3.68 ± 0.039			30	4.45 ± 0.715	
	16	11.4 ± 0.065			10	44.9 ± 25.6	
	17	95.7 ± 0.502		hybrid **D**	72	0.858 ± 0.0257	0.638
hybrid **A**	49	2.81 ± 0.574	0.921		28	5.69 ± 0.0985	
	16	0.598 ± 0.928		polymer **13**	33	0.315 ± 0.0173	0.907
	19	19 ± 4.36			33	1.06 ± 0.0252	
	17	53.5 ± 11.3			34	5.12 ± 0.038	
				hybrid **E**	36	0.825 ± 0.129	0.918
hybrid **B**	60	0.485 ± 0.114	1.018		22	5.49 ± 0.653	
	20	3.42 ± 0.51			42	160 ± 16.3	
	20	134 ± 26.3		hybrid **F**	58	1.25 ± 0.0234	1.055
polymer **11**	43	1.33 ± 0.0174	0.742	27		9.74 ± 0.0924	
	25	0.478 ± 0.0216			15	82.8 ± 1.1	
	14	7.31 ± 0.0749					

[a] When the χ value is low, the agreement between the calculated fit and the experimental curve is very good.

The common precursor of the target carbazole-containing polymers **10** and **11** originates from the known 2,7-dibromocarbazole, **1**. The incorporation of the 3-carbon and 4-carbon sulfonate-containing chain at the *N*- position of the carbazole was performed in good yields according to a procedure outlined by Zong and collaborators[11] (Scheme 3). The procedure uses propanesultone and butanesultone (Scheme 3), hence forming the sodium 3-(2,7-dibromo-carbazole)propane-1-sulfonate, **4**, and sodium 4-(2,7-dibromocarbazole)butane-1-sulfonate, **5**, intermediates, respectively.

The polymer formation of **10** and **11** is then performed in good yields from the condensation of precursors **4** and **5**, respectively, with *p*-phenyldiboronic acid in the presence of a Pd catalyst (Scheme 4). The resulting polymers turn out to be weakly soluble; therefore, solvents like DMSO had to be employed for characterization (i.e., ^{1}H NMR). The low solubility also prevents gel permeation chromatography analysis (GPC). The two polymers are found to be mainly amorphous according to X-ray diffraction (XRD) analyses, but broad peaks are observed, indicating the presence of some crystallinity in the bulk materials (Figure 1).

Polymer **13** is synthesized in six steps from *p*-bromo(methoxy)benzene and precursor **5** (Scheme 5). The former starting material is converted in low yield into intermediate **7**, which contains a soluble *n*-octane chain, from the corresponding Grignard reagent. Compound **7** is then transformed into the corresponding alcohol, intermediate **8**, using the tribromoborane reactant. Compound **8** is used as a protecting group in the synthesis of the target polymer **13**, but also the better solubility of this octane-containing group eases the following syntheses. In parallel, compound **5** is chlorinated in good yield from the phosphorus pentachloride reagent, to provide the corresponding sulfonyl chloride derivative **6**. The nucleophilic coupling of **6** and **8** occurs in the presence of a base to generate intermediate **9**. The polymerization of **9** proceeds in good yield in the presence of a stoichiometric amount of bis(cyclooctadiene)nickel(0) to form the neutral polymer **12**. The anionic polymer **13** is subsequently prepared in excellent yield from the deprotection of the sulfonyl function using a strong base. DMF as the solvent was necessary to solubilize the polymer prior to the reaction. The solubility of the resulting polymers **12** and **13** was good enough for ^{1}H NMR characterization in DMF and DMSO, respectively. Moreover, the materials turn out to be amorphous similarly to polymers **10** and **11** (Figure 1). Attempts were made to extract the Mw and Mn of polymer **12** in DMF from GPC and light-scattering methods, but the polymer has a strong tendency to form aggregates even after ultrafiltration of the material. Higher-temperature conditions (60 °C) were also used but without success. No reliable data were extracted.

2. Characteristics of the Cationic Organometallic Polymers. The two known organometallic polymers, $([Pt_2(dppm)_2(CNC_6Me_4NC)](BF_4)_2)_n$, and $([Ag(dmb)_2]BF_4)_n$, were selected for several reasons. First, the comparison between Na^+ (of the uncoupled carbazole-containing polymers described above), Ag^+, and Pt^+ allows one to address the heavy-atom effect on the emission properties of the resulting hybrid materials. Second, they exhibit "rigid stick"

structures (Figure 2), allowing one to address the distances between the positive charges.[5,6,14]

The third reason for these selections stems from the polymer (solid state)/oligomer (solution) equilibrium.[15] Indeed, this equilibrium is very useful because it provides an adaptability of the polycationic chain to adjust its chain length in order to match that of the organic polymers, which we suspect to be polydispersed.[16,17]

Fourth, the $([Ag(dmb)_2]^+)_n$ polymer usually exists with dmb ligands in its U shape, as illustrated in Figure 2 and Scheme 6. However, very subtle changes in experimental conditions such as the solvent are strong enough to provoke the isomerization of the dmb ligand from the U shape to a Z shape (Scheme 6).[18] The isomerization process was found to be totally reversible (i.e., $(Ag(U\text{-}dmb)^+)_n = (Ag(Z\text{-}dmb)(U\text{-}dmb)^+)_n = (Ag(Z\text{-}dmb)^+)_n$), also illustrating the equilibrium between oligomers of different lengths in solution. The resulting isomeric polymers exhibit different distances between the positive charges (Ag^+; Scheme 6). This feature is interesting because it provides another source of adaptability of the polycationic polymer with the organic polyanionic ones.

Fifth, the $([Pt_2(dppm)_2(CNC_6Me_4NC)](BF_4)_2)_n$ and $([Ag(dmb)_2]BF_4)_n$ polymers are yellow[16] and white,[5,6] respectively, exhibiting singlet and triplet energy levels that can be placed either below or above the singlet and triplet manifolds of the polycarbazole polymers. This feature provides the possibility of observing energy transfer either from the organic polymers to the organometallic ones, or vice versa. Details are provided below. In addition, whereas the carbazole unit is known to be a good photoinduced electron donor,[19] the low-valent d^{10} $([Ag(dmb)_2]BF_4)_n$ and d^9-d^9 $([Pt_2(dppm)_2(CNC_6Me_4NC)](BF_4)_2)_n$ polymers are not prone to act as good electron acceptors. Moreover, it was demonstrated that $([Ag(dmb)_2]^+)_n$ is not a donor for photoinduced electron transfer due to the high-energy Ag^+/Ag^{2+} redox couple.[14,20] Thus, the possibility of photoinduced electron transfers between the two polymers inside the hybrid materials is reasonably ruled out.

The coupling of the polyanionic and polycationic polymers induces strong electrostatic interactions between the chains, so the distance between charges hypothetically plays an important role in the stability of the resulting hybrid. On the basis of qualitative computer modeling (PC-Model), the separations between the negative charges taken as the N···N distances were estimated (Scheme 7). The theoretical parallel stacking of the anionic (Scheme 7) and cationic polymers shown in Figure 2 and Scheme 6 predicts obvious mismatches, except for one combination. The library of distances in the polyanions for two repetitive charged units is 25.3 and 16.1 Å, while that for the polycations is 9.0, 17.2, 20.2, and 21.0 Å. A reasonable matching combination would be polymer **13** with the $([Ag(dmb)_2]^+)_n$ polymer (16.1 vs 17.2 Å) for parallel stacking. In any case, the presence of a C_6H_4 group in the chain, and a $(CH_2)_3SO_3$ or a $(CH_2)_3SO_3$ pendent chain, allows more adaptability in order to favor the ion pair formation in the solid.

In a previous work,[14] the $([M(dmb)_2]^+)_n$ polymers (M = Ag, Cu) were investigated in the presence of mixed-valent tetracyanoquinodimethane, $TCNQ^{n-}$, made from the mixing of $TCNQ^0$ and $TCNQ^{1-}$. One X-ray structure was solved where layers of stacked parallel $([Ag(dmb)_2]^+)_n$ polymers alternate with a regular "carpet" of $(TCNQ^{n-})_m$, inducing conductivity. The "center-to-center" axis in the $(TCNQ^{n-})_m$ chain exhibits a slipped linear stack forming angle of about 50° with the $([Ag(dmb)_2]^+)_n$ polymers. This angle is different from 0° because of a mismatch with the repetitive units of the polycations and anions carrying the same charge. It is anticipated that a similar situation will occur in these hybrid materials.

3. Syntheses of the Hybrid Materials. The coupling of the polymers **10**, **11**, and **13** with the $([Pt_2(dppm)_2(CNC_6Me_4NC)](BF_4)_2)_n$ and $([Ag(dmb)_2]BF_4)_n$ polymers provides six possible combinations. They are designated as hybrids **A**−**F** (Table 1).

Their preparations proceed from the slow mixing of an anionic carbazole-containing polymer solution in DMSO with an acetonitrile solution containing the cationic organometallic polymer. The quantity is adjusted to have exactly the same number of negative and positive charges on the polymers. The two-day stirring is selected in order to allow the polycationic polymer to adjust its length and conformation (if any) to fit that of the anionic carbazole-containing polymer. After precipitation, the multiple washings with methanol allowed for the removal of the DMSO solvent and the $NaBF_4$ salt. The hybrid materials exhibit very weak solubility, similar to those of the organic ones described above. IR spectroscopy (Figure 3) reveals the absence of a peak attributable to acetonitrile (either coordinated or uncoordinated), which exhibits ν(CN) at a different frequency than the ν(NC) ones of the polymers, and $NaBF_4$. The $Pt_2(dppm)_2(CNR)_2^{2+}$ core remains intact, as demonstrated by IR and Raman spectroscopy.

The presence of a center of inversion makes the symmetric and asymmetric ν(NC) modes Raman- and IR-active, respectively, only for an approximate local C_2 point group, as illustrated in hybrids **B** and **D** (Figure 3). Indeed, the Raman-active mode is observed at 2165 cm^{-1}, whereas the IR-active mode is noted at 2153 cm^{-1} for both cases. Because of the low solubility, both ^1H and ^{13}C NMR spectra were recorded in the solid state (MAS). Examples are shown in Figure 4. The remainder is placed in the Supporting Information. The NMR MAS spectra for all six hybrids are almost the sum of

(14) Fortin, D.; Drouin, M.; Harvey, P.D. *Inorg. Chem.* **2000**, *39*, 2758.
(15) (a) Sicard, S.; Bérubé, J.-F.; Samar, D.; Massaoudi, A.; Lebrun, F.; Fortin, J.-F.; Fortin, D.; Harvey, P. D. *Inorg. Chem.* **2004**, *43*, 5321. (b) Turcotte, M.; Harvey, P. D. *Inorg. Chem.* **2002**, *41*, 1739.
(16) Bérubé, J.-F.; Gagnon, K.; Fortin, D.; Decken, A.; Harvey, P. D. *Inorg. Chem.* **2006**, *45*, 2812.
(17) Fortin, D.; Drouin, M.; Harvey, P. D. *J. Am. Chem. Soc.* **1998**, *120*, 5351.
(18) (a) Ohkita, H.; Benten, H.; Anada, A.; Noguchi, H.; Kido, N.; Ito, S.; Yamamoto, M. *Phys. Chem. Chem. Phys.* **2004**, *6*, 3977. (b) Chen, J.; Chen, J.; Li, S.; Zhang, L.; Yang, G.; Li, Y. *J. Phys. Chem. B* **2006**, *110*, 4663. (c) Zotti, G.; Schiavon, G.; Zecchin, S.; Morin, J. F.; Leclerc, M. *Macromol.* **2002**, *35*, 2122.
(19) Fortin, D.; Harvey, P. D. *Coord. Chem. Rev.* **1998**, *171*, 351.
(20) Tirapattur, S.; Belletête, M.; Drolet, N.; Leclerc, M.; Durocher, G. *Chem. Phys. Lett.* **2003**, *370*, 799.

the corresponding spectra of both starting materials, indicating that both polymers are present in the resulting materials.

Two of the six hybrids were investigated by XRD (Supporting Information; see hybrids **B** and **E**). The materials are found primarily to be amorphous, although medium-sharp features are observed. These features appear more intense and sharper than that depicted in the XRD traces of polymers **10**−**13** (Figure 1). These features indicate the presence of crystalline regions in the larger hybrids. This may be due to the desired strong electrostatic interactions between the polymer chains of different charges.

4. Fluorescence and Phosphorescence Spectra. The energy diagrams including both the anionic conjugated organic and cationic organometallic polymers are constructed using the fluorescence (∼460) and phosphorescence (∼585 nm) data included in this work (polycarbazoles), and the literature data reported by our group for the organometallic polymers (data decribed below).

For the colorless $([Ag(dmb)_2]^+)_n$ polymer, the absorption spectra exhibit a maximum at 205 nm assigned to a charge-transfer transition (d^{10} $Ag^+ \rightarrow \pi^*$-CN) in acetonitrile.[5,6] This band places the singlet state well above those of the polycarbazoles. Similarly, the solid-state emission spectra exhibit a strong and long-lived luminescence centered at 515 nm, somewhere between the solid-state fluorescence and phosphorescence bands of the investigated polycarbazoles in this work. This luminescence, which exhibits a large Stokes shift ($<30\,000$ cm^{-1}) and a long lifetime (∼100 μs), is known to be associated with an emission arising from a triplet state. Hence, this state is placed above the triplet state of the polycarbazoles.

Similarly, the yellow-colored M_2-bonded $([Pt_2(dppm)_2](CNC_6Me_4NC)^{2+})_n$ polymer exhibits a low-energy absorption band at 344 nm in butyronitrile at 298 K associated with the symmetry-allowed $d\sigma d\sigma^*$ transition typical for d^9-d^9 species.[17] On the basis of density functional theory (DFT) molecular orbital analysis, this electronic transition is not the lowest energy one, but a symmetry-forbidden charge transfer (CT) of π-ArN≡C to $d\sigma^*$ is computed.[17] The emission band for this polymer is rather weak and is found to be much red-shifted at 732 (solid state, 77 K), 727 (solid state, 298 K), and 715 nm (butyronitrile, 77 K).[17] The Stokes shift is also large, as well as the lifetime (∼3 μs), meaning that this band is also attributable to a triplet state. All in all, this state clearly lies below the triplet state of the polycarbazoles. The location of the corresponding but symmetry-forbidden low-energy singlet CT state is not known, as its corresponding absorption or emission was not observed or predicted using time-dependent DFT methods. [17] Nonetheless, the fact that the fluorescence bands of the polycarbazoles in the hybrid materials containing this Pt-containing polymer are strongly quenched (more than what spin−orbit coupling would induce, see below) suggests that this optically silent CT singlet state must lie below that of the polycarbazoles and that quenching is due to efficient singlet−singlet energy transfer. On the basis of all of these observations, the energy diagrams for the two families of hybrids can be constructed (Figure 5) and used for the description of the experimental results.

Figures 6 and 7 exhibit the emission and excitation spectra of polymers **10**, **11**, and **13** and hybrids **A**−**F** in the solid state at 298 K. The 77 K spectra are also recorded, and the corresponding spectra are placed in the Supporting Information, as they bear the same information. The fluorescence bands of the polycarbazoles are easily depicted in polymers **10**, **11**, and **13** in the 450 nm region. The short nansecond time scale measured for these emissions supports this assignment. The excitation spectra (in red) exhibit a strong and narrow peak just slightly blue-shifted beside the high-energy shoulder of the fluorescence band. The fluorescence and excitation band shapes and positions of polymer **10** provide a "finger print" for the analysis of the corresponding emission of the hybrid materials. In addition to the fluorescence, a weak phosphorescence appearing as a long tail is visible in the 550−650 nm range. The long emission lifetimes (microseconds, presented below) are consistent with this assignment.

The $([Ag(dmb)_2]^+)_n$-containing materials (hybrids **A**, **C**, and **E**) exhibit the spectroscopic features associated with the fluorescence of the polycarbazoles at about 450 nm, but the relative phosphorescence intensity is strikingly increased. This behavior is indicative of a heavy atom effect (Na vs Ag), and this proposal is supported by the observation of an even stronger phosphorescence of the polycarbazole unit for hybrid **E** (Ag vs Pt). There is no direct evidence for the generally strong emission of the organometallic polymer $([Ag(dmb)_2]^+)_n$ at 515 nm.[5,6] In an attempt to find this emission, time-resolved emission spectroscopy was employed (Figure 8) using the known argument that different species exhibit different excited-state lifetimes. This slower-decaying $([Ag(dmb)_2]^+)_n$ emission was indeed discriminated under the more intense fluorescence of the polycarbazole. One question which arises is as follows: why are both the intensity and the lifetime (on the nanosecond time scale rather than the microsecond) much smaller than those for the simple $([Ag(dmb)_2]Y)_n$ polymers (Y = BF_4^-, PF_6^-, ClO_4^-, $CH_3CO_2^-$, NO_3^-)?[5,6] The answer lies in the triplet−triplet energy transfer, as described in Figure 5. On the basis of this diagram, the population of units in the polycarbazole chains lying in the triplet state is first accentuated by the increase in intersystem crossing from the heavy atom effect. In addition, triplet−triplet energy transfer can occur from the T_1 state of $([Ag(dmb)_2]^+)_n$ to the T_1 state of the polycarbazole. The former state can be fed by the S_1 state of the polycarbazole.

This proposal is supported by the even higher phosphorescence intensities for hybrids **C** and **E**, where the heavy atom is still the same (Ag). So another process is taking place and can only be triplet−triplet energy transfer. This proposal is further supported by hybrids **D** and **F**, where both the fluorescence and phosphorescence are very weak, a low intensity that can only be explained by an efficient energy-transfer processes, as described in Figure 5 (bottom). Again, the organometallic $([Pt_2(dppm)_2]CNC_6Me_4NC)^{2+})_n$ polymer exhibits a low-lying triplet excited state that can act as an

energy acceptor. Strong intersystem crossing due to Pt accentuates the funnelling of this energy through this lower-energy triplet state. The relative ratios of the fluorescence and phosphorescence intensities are different for the hybrids of Figure 6 versus those of Figure 7. The reason for different efficiencies in the energy transfers is still unknown to us.

Emission Decay Traces and Lifetimes. The related poly(*N*-octyl-2,7-carbazole; POC) was investigated by Durocher and collaborators as thin films.[20] In their work, the authors demonstrated that POC exhibited a linear fluorescence decay trace in solution, but the multiexponential model had to be employed to describe the fluorescence decay as a thin film. They also estimated qualitatively the fluorescence quantum yield (Φ_F) in the film using Φ_F and τ_F in solution (Φ_F (film) ~40%). In this work, the hybrid materials are not soluble and were analyzed by emission lifetime decay traces only in the solid state. We employed the ESM (multiexponential method)[21] since we find that better fits are obtained in comparison with double, triple, and quadruple models. This method allows for computation of up to 200 lifetimes along with relative intensity, so the data are represented as graphs for convenience. The maximum in the graphs of the relative intensity as a function of lifetime represents the most probable lifetime. The width of this distribution is related to the curvature of the decay trace on the log scale. A single exponential decay gives a narrow distribution. For comparison purposes, we investigated the conjugated *N*-hexyl-3,6-bisethynylcarbazole model in the solid state as well (Scheme 8).

The distribution of lifetime exhibits a maximum at ~5.2 ns and a full-width at half-maximum (fwhm) of ~0.4 ns (Figure 9). This is a moderate distribution. For the *N*-butyl-carbazol-3,6-diyl trimer, the maximum of the distribution of lifetime has a value of ~4.7 ns with a fwhm of ~0.7 ns (Figure 9).

Polymers **10**, **11**, and **13** exhibit maxima in the graph of the lifetime distributions at 0.83, 0.92, and 0.73 ns (Figure 10), with fwhm values of ~0.25, 0.50, and ~0.20 ns, respectively (Table 2). The most probable fluorescence lifetimes for the polymers are shorter than that of the model compounds. This behavior was also noted by Durocher and collaborators for POC and is obviously due to the polymeric nature of the material. This nonexponential behavior of the emission decays for other polymers was also investigated by one of us previously (P.D.H.)[6,22] and is found to be due to an excitonic process (i.e., energy delocalization similar to excimers with variable lengths). A clear relationship between the length of the oligomers and the amplitude of the curvature of the decay trace was also demonstrated.[22] In this work, clear evidence for excitonic behavior is observed. In general, nonexponential decays are difficult to interpret.

Interestingly, in this work, we did not observe a decrease in the carbazole-centered τ_F in the hybrids while expecting one based on the external heavy atom effect and energy-transfer processes described above. One way to provide a possible explanation is that the rate for exciton migration must be faster than the intersystem crossing (due to the external heavy atom effect) and interpolymer chain energy-transfer rate constants, so that the dominant exciton signature in the nonexponential decay traces hides these two slower processes. The rate for exciton migration is well-known to be faster than energy transfers as well exemplified in antenna devices in photosynthetic bacteria.[23]

The phosphorescence decays were also analyzed at 77 K (for better intensity), and similar observations were made. The decay traces (Supporting Information) are not monoexponential, and all of them required at least two components, generally best described as one or two short-lived components of high intensity and a slower one that is not generally of low intensity. Table 3 reports the decay analyses where the results from the lowest χ were obtained (i.e., best fit). The phosphorescence lifetime of the strongest component for the model compound *N*-hexyl-3,6-bisethynylcarbazole (~2 ms) is longer than that for polymers **10**−**12**, again stressing the effect of the polymeric and solid-state nature of the materials on τ_P. Because of the multiexponential nature of the decay traces, the presence of an excitonic process (energy delocalization) is suspected to be taking place. Other literature examples of the exciton in the triplet state exist.[6] We are not able to assign with certainty the emission lifetimes of the organometallic polymer. On the basis of the time-resolved spectra described above, the lifetime must be longer than that of the organic carbazole-containing polymers.

Conclusion

Novel mixed cation/anion polymer-containing materials, where the polymers are conjugated carbazole-containing polymers, bearing anionic side chains, and the organometallic polymers, where the state of charge of the metal makes them polycations, were prepared and characterized. Because of the lack of solubility, these new hybrid materials were solely investigated in the solid state. Evidence was found for a heavy atom effect (from the Ag and Pt metals), where a large increase of the phosphorescence intensity of the carbazole-containing polymers indicated interchain contacts across the materials. These interactions were further illustrated from the evidence of interchain energy transfers. All emission decay traces are found to be polyexponential, indicating the presence of an exciton (i.e., excitation energy delocalization).[6] Because through-space triplet energy transfer between the organic and organometallic polymer chains is observed, and this process occurs solely via a double-electron exchange (Dexter mechanism), it becomes obvious that a single photoinduced electron transfer is also possible for related polymers (i.e., structurally similar) that exhibit thermodynamically favorable redox properties. Therefore, this property "opens the door" to a possible design of hybrid cation/anion photoconduction polymer

(21) James, D. R.; Ware, W. R. *Chem. Phys. Lett.* **1986**, *126*, 7.
(22) Harvey, P. D.; Fournier, É. *ACS Symp. Ser.* **2006**, *928*, 472.
(23) *Light-Harvesting Antennas in Photosynthesis; Advances in Photosynthesis and Respiration*, Green, B. R.; Parson, W. W., Eds.; Kluwer Academic Publishers: Boston, 2003; Vol *13*.

materials and solar cells. The ideal hybrid materials can be obtained by the incorporation of longer soluble side chains for easier characterization and for the possibility of polymer film formation.

Acknowledgment. This research was supported by the Natural Sciences and Engineering Research Council of Canada (NSERC) and Le Fonds Québécois de la Recherche sur la Nature et les Technologies (FQRNT). The authors thank Dr. Victor V. Terkikh for the NMR measurements with access to the 900 MHz NMR spectrometer, which was provided by the National Ultrahigh Field NMR Facility for Solids (Ottawa, Canada), a national research facility funded by the Canada Foundation for Innovation, the Ontario Innovation Trust, Research Quebec, the National Research Council Canada, and Bruker Biospin and managed by the University of Ottawa (www.nmr900.ca). The Natural Sciences and Engineering Research Council of Canada (NSERC) is acknowledged for a Major Resources Support grant.

Supporting Information Available: Additional figures are provided. This material is available free of charge via the Internet at http://pubs.acs.org.

IC801461J